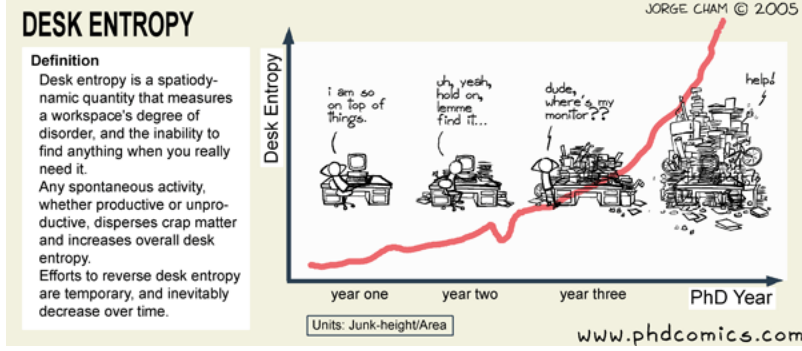
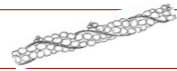


3. biopolymers - entropy



me239 mechanics of the cell

1

biopolymers

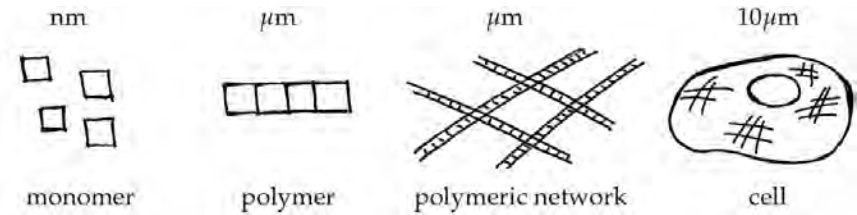


Figure 3.1. Biopolymers. Characteristic length scales on the cellular and subcellular level.

3.1 biopolymers - motivation

2

the cytoskeleton

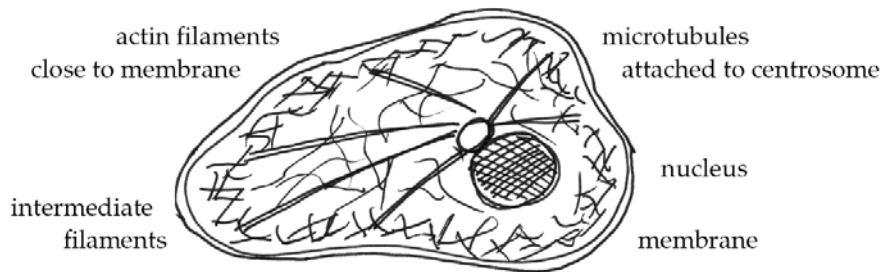


Figure 1.3. Eukaryotic cytoskeleton. The cytoskeleton provides structural stability and is responsible for force transmission during cell locomotion. Microtubules are thick hollow cylinders reaching out from the nucleus to the membrane, intermediate filaments can be found anywhere in the cytosol, and actin filaments are usually concentrated close to the cell membrane.

3.1 biopolymers - motivation

3

actin filaments

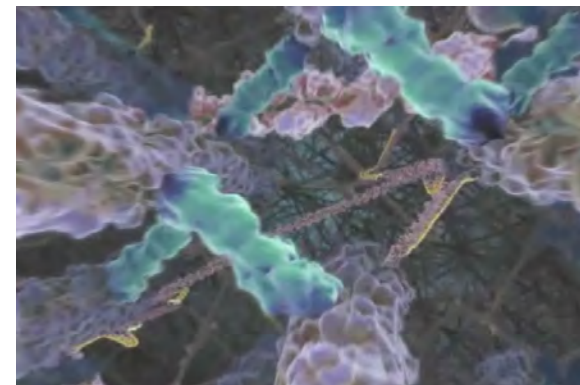


Figure 1.4.1 Actin filaments form tight parallel bundles which are stabilized by cross-linking proteins. Deeper in the cytosol the actin network adopts a gel-like structure, stabilized by a variety of actin binding proteins.

the inner life of a cell, viel & lue, harvard [2006]

3.1 biopolymers - motivation

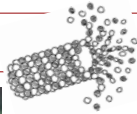
4

microtubules



Figure 1.4.3 The cytoskeleton includes a network of microtubules created by the lateral association of protofilaments formed by the polymerization of tubulin dimers.

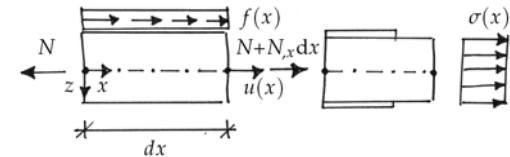
the inner life of a cell, viel & lue, harvard [2006]



3.1 biopolymers - motivation

5

axial deformation - tension



$$EA u_{,xx} + f = 0 \quad \text{with} \quad EA \dots \text{axial stiffness}$$

$$\text{cross section area } A = \pi r^2$$

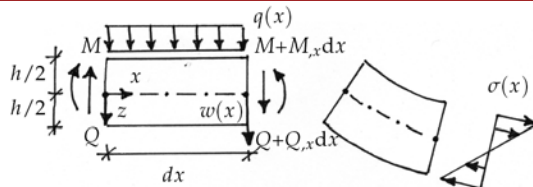
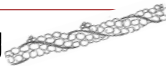
	r	A	E	EA
microtubule	12.5 nm	491 nm ²	1.9·10 ⁹ N/m ²	93·10 ⁻⁸ N
intermediate filament	5.0 nm	79 nm ²	2.0·10 ⁹ N/m ²	15·10 ⁻⁸ N
actin filament	3.5 nm	39 nm ²	1.9·10 ⁹ N/m ²	7·10 ⁻⁸ N

Table 3.1: Axial stiffness EA of major constituents of cytoskeleton: microtubules, intermediate filaments and actin filaments

3.2 biopolymers - energy

6

transverse deformation - bending



$$q = EI w_{,xxxx} \quad \text{with} \quad EI \dots \text{bending stiffness}$$

$$\text{for circular cross sections } I = \pi r^4 / 4$$

	r	I	E	EI
microtubule	12.5 nm	19,175 nm ⁴	1.9·10 ⁹ N/m ²	364·10 ⁻²⁵ Nm ²
intermediate filament	5.0 nm	491 nm ⁴	2·10 ⁹ N/m ²	10·10 ⁻²⁵ Nm ²
actin filament	3.5 nm	118 nm ⁴	1.9·10 ⁹ N/m ²	2·10 ⁻²⁵ Nm ²

Table 3.2: Bending stiffness of major constituents of cytoskeleton: microtubules, intermediate filaments and actin filaments

3.2 biopolymers - energy

7

free energy - energy and entropy



$$\psi = W - TS \quad \dots \text{free energy}$$

$$\bar{W} = \bar{W}(\epsilon) \quad \dots \text{strain energy}$$

$$T = 300K \quad \dots \text{absolute temperature}$$

$$S = k \ln(p) \quad \dots \text{Boltzmann equation}$$

$$k = 1.38 \cdot 10^{-23} \text{ J/K} \dots \text{Boltzmann constant}$$

$$\psi = W - TS \approx -TS = -Tk \ln(p)$$

3.3 biopolymers - entropy

8



ludwig boltzmann [1844-1906], zentralfriedhof vienna

3.3 biopolymers - entropy

9

uncorrelated chains - freely jointed chain

bonds	configurations	probability $p(r/L)$
$N = 1$	$2^1 = 2$	1 - 1
$N = 2$	$2^2 = 4$	1 - 2 - 1
$N = 3$	$2^3 = 8$	1 - 3 - 3 - 1
$N = 4$	$2^4 = 16$	1 - 4 - 6 - 4 - 1
$N = 5$	$2^5 = 32$	1 - 5 - 10 - 10 - 5 - 1
$N = 6$	$2^6 = 64$	1 - 6 - 15 - 20 - 15 - 6 - 1

Table 3.4: Probability distribution for configurations of one-dimensional chain with N bonds

$$N \rightarrow \infty \quad \begin{aligned} p^{1\text{dim}} &= p_0 \exp\left(-\frac{1}{2} N r^2/L^2\right) \quad \dots \text{1d probability density} \\ p^{3\text{dim}} &= p_0 \exp\left(-\frac{3}{2} N r^2/L^2\right) \quad \dots \text{3d probability density} \end{aligned}$$

3.3 biopolymers - entropy

10

uncorrelated chains - freely jointed chain

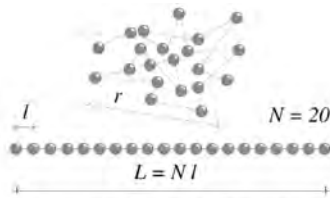


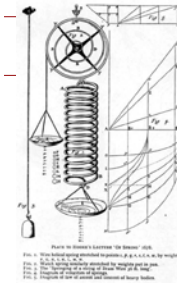
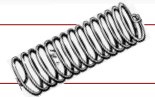
Figure 3.8: Uncorrelated chain. Kinematics of the freely jointed chain model with number of bonds N , bond length l , contour length $L = Nl$, and end-to-end length r .

$$\begin{aligned} p &= p_0 \exp\left(-\frac{3}{2} N r^2/L^2\right) \quad \dots \text{Gaussian probability density} \\ \psi^{\text{fjc}} &= \psi_0^{\text{fjc}} + k T N \frac{3}{2} \frac{r^2}{L^2} \quad \dots \text{Gaussian free energy} \\ f^{\text{fjc}} &= \frac{\partial \psi^{\text{fjc}}}{\partial (r/L)} = k T N 3 \frac{r}{L} \quad \dots \text{Gaussian force-stretch relation} \end{aligned}$$

3.3 biopolymers - entropy

11

example - entropic spring

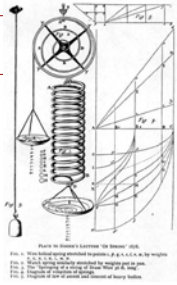


"The power of any spring is in the same proportion with the tension thereof: that is, if one power stretch or bend it one space, two will bend it two, and three will bend it three, and so forward. Now as the theory is very short, so the way of trying it is very easy."

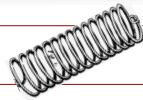
Robert Hooke [1678] De Potentia Restitutiva

3.3 biopolymers - entropy

12



example - entropic spring



"The power of any spring is in the same proportion with the tension thereof: that is, if one power stretch or bend it one space, two will bend it two, and three will bend it three, and so forward. Now as the theory is very short, so the way of trying it is very easy."

Robert Hooke [1678] De Potentia Restitutiva

Entropic spring Do you remember Hooke's law for a linear elastic spring? For that simple model, the spring stiffness k could be calculated as the second derivative of the spring energy $\psi = \frac{1}{2} k^{spr} u^2$ such that $\partial^2 \psi / \partial u^2 = k^{spr}$. We can do the same thing for the entropic polymer. The second derivative of its energy $\psi^{fc} = \psi_0^{fc} + k T N \frac{3}{2} r^2 / L^2$ with respect to r gives us $\partial^2 \psi / \partial r^2 = 3 k T N / L^2$. This is the equivalent stiffness of a spring that had the same stretch resistance as the biopolymer modeled with as an uncorrelated Gaussian chain. The biopolymer can thus be understood as an entropic spring with the spring stiffness $3 k T N / L^2$.

3.3 biopolymers - entropy

13

uncorrelated chains - freely jointed chain

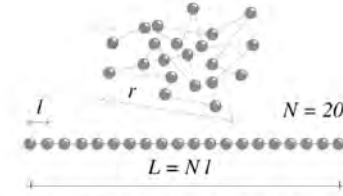


Figure 3.8: Uncorrelated chain. Kinematics of the freely jointed chain model with number of bonds N , bond length l , contour length $L = Nl$, and end-to-end length r .

$$p = p_0 \exp(-N \mathcal{L}^{-1} r/L - N \ln(\mathcal{L}^{-1} / \sinh(\mathcal{L}^{-1}))) \quad \dots \text{Langevin probability density}$$

$$\psi^{fc} = \psi_0^{fc} + k T N (\mathcal{L}^{-1} r/L + \ln(\mathcal{L}^{-1} / \sinh(\mathcal{L}^{-1}))) \quad \dots \text{Langevin free energy}$$

$$f^{fc} = \frac{\partial \psi^{fc}}{\partial (r/L)} = k T N \mathcal{L}^{-1} \quad \dots \text{Langevin force-stretch relation}$$

3.3 biopolymers - entropy

14

correlated chains - wormlike chain

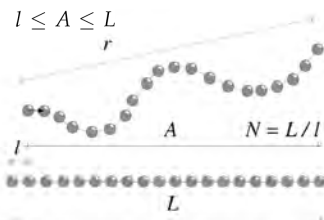


Figure 3.9: Correlated chain. Kinematics of the wormlike chain model with number of bonds N , bond length l , contour length $L = Nl$, end-to-end length r , and persistence length A .

$$\psi^{wlc} = \psi_0^{wlc} + \frac{k T}{4 A L} \left[2 \frac{r^2}{L^2} + \frac{1}{1 - r/L} - \frac{r}{L} \right] \quad \dots \text{free energy}$$

$$f^{wlc} = \frac{\partial \psi^{wlc}}{\partial (r/L)} = \frac{k T}{4 A L} \left[4 \frac{r}{L} + \frac{1}{[1 - r/L]^2} - 1 \right] \quad \dots \text{force-stretch relation}$$

3.3 biopolymers - entropy

15

freely jointed chain vs wormlike chain

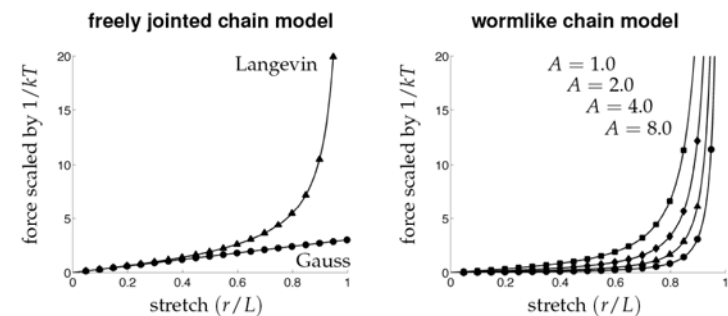
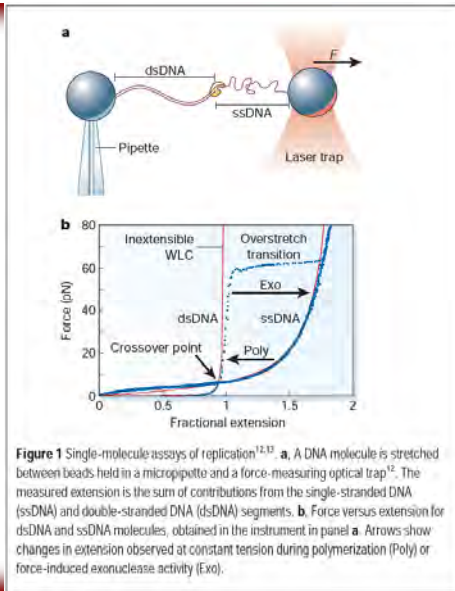


Figure 3.10: Force stretch relation of freely jointed chain models, left, and wormlike chain models, right. In the small strain limit, the Gaussian chain and the Langevin chain display an identical behavior. The Gaussian chain is linear throughout the entire regime whereas the Langevin chain stiffens significantly close to the locking stretch at $r/L = 1$. Different persistence length produce a different force stretch response of the wormlike chain model.

3.3 biopolymers - entropy

16



bustamante, bryant, smith [2003]

3.3 biopolymers - entropy

17

concept of persistence length



biopolymer	configuration	A [nm]
spectrin	double-stranded filament	10 – 20
DNA	double helix	51 – 55
F-actin	filament	$10 - 20 \cdot 10^3$
microtubules	13 protofilaments	$1 - 6 \cdot 10^6$

Table 3.5: Experimentally measured persistence lengths of different biopolymers

3.3 biopolymers - entropy

18

concept of persistence length



- stiffer filaments are straighter \propto bending stiffness EI
- cooler filaments are straighter \propto inverse temperature kT

$$A = \frac{EI}{kT} \quad \dots \quad \text{persistence length} \quad l \leq A \leq L$$

	r	E	EI	$A = [EI]/[kT]$
microtubule	12.5 nm	$1.9 \cdot 10^9 \text{N/m}^2$	$364 \cdot 10^{-25} \text{Nm}^2$	8.800 mm
intermediate filament	5.0 nm	$2 \cdot 10^9 \text{N/m}^2$	$10 \cdot 10^{-25} \text{Nm}^2$	0.240 mm
actin filament	3.5 nm	$1.9 \cdot 10^9 \text{N/m}^2$	$2 \cdot 10^{-25} \text{Nm}^2$	0.048 mm

Table 3.6: Persistence lengths of major constituents of cytoskeleton at room temperature: microtubules, intermediate filaments and actin filaments

3.3 biopolymers - entropy

19

concept of persistence length



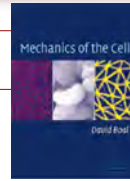
$$A = \frac{EI}{kT} \quad \dots \quad \text{persistence length}$$

- informally, for pieces of the polymer that are **shorter** than the persistence length, the molecule behaves rather like a **flexible elastic rod**, while for pieces of the polymer that are much **longer** than the persistence length, the properties can only be described statistically, like a three-dimensional **random walk**
- formally, the persistence length is defined as the **length over which correlations** in the direction of the **tangent are lost**
- the persistence length is the **distance** which we should travel from one end of the chain **to bend it 90 degrees**

3.4 biopolymers - entropy

20

concept of persistence length



$$A = \frac{EI}{kT} \quad \dots \quad \text{persistence length}$$

one way of **quantifying** the amplitude of the shape **fluctuations** at finite temperature is finding the typical distance along the rod over which it undergoes a significant change in direction: flexible rods change direction over shorter distances than stiff rods. this length scale must be **directly proportional to** the flexural rigidity EI and **inversely proportional to** the temperature kT . in fact, the combination of EI/kT has the units of a length, and is defined as the persistence length of the filament.

suggested reading: 2.1 filaments in the cell / 2.5 elasticity and cellular filaments
mechanics of the cell, boal [2002]

3.4 biopolymers - entropy

21

concept of persistence length



$$A = \frac{EI}{kT} \quad \dots \quad \text{persistence length}$$

- the persistence length is a measure of the length scale over which a **polymer remains roughly straight**
- the persistence length is a measure of the **competition between** the **entropic** parts of the free energy randomizing the orientation of the polymer and the **energetic** cost of bending.
- the persistence length is the scale over which the **tangent-tangent correlation function decays** along the chain

suggested reading: 8.2 macromolecules as random walks / 10.2.2 beam theory and the persistence length
physical biology of the cell, phillips, kondev, theriot [2009]

3.4 biopolymers - entropy

22

example - persistence length of spaghetti



Persistence length of spaghetti Try to guess the persistence length A of spaghetti at room temperature. Would it be smaller than the spaghetti length, approximately the same or larger? Assume spaghetti have a diameter of $d = 2\text{mm}$ and a Young's modulus of $E = 1 \cdot 10^8 \text{J/m}^3 = 1 \cdot 10^8 \text{N/m}^2$.

example - persistence length of spaghetti



Persistence length of spaghetti Try to guess the persistence length A of spaghetti at room temperature. Would it be smaller than the spaghetti length, approximately the same or larger? Assume spaghetti have a diameter of $d = 2\text{mm}$ and a Young's modulus of $E = 1 \cdot 10^8 \text{J/m}^3 = 1 \cdot 10^8 \text{N/m}^2$. The temperature and the Boltzmann constant are $T = 300\text{K}$ and $k = 1.38 \cdot 10^{-23} \text{J/K}$. The persistence length of spaghetti is $A = [EI] / [kT]$, with the moment of inertia $I = [\pi r^4] / 4$ with $r=1\text{mm}$. Accordingly, $A = [1 \cdot 10^8 \text{N/m}^2 \pi \text{mm}^4] / [4 \cdot 1.38 \cdot 10^{-23} \text{J/K} \cdot 300 \text{K}] = 1.8 \cdot 10^{16} \text{m}$. An uncooked spaghetti changes its direction at length scales of the order of $A = 1.8 \cdot 10^{13} \text{km}$. Is that a lot? Well, yes, that's quite stiff if you consider that the distance from the earth to the moon is about $3.8 \cdot 10^5 \text{km}$!



a cooked spaghetti has a persistence length on the order of 1-10 cm

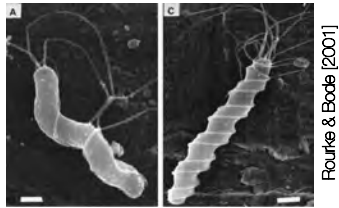
3.3 biopolymers - entropy

23

3.3 biopolymers - entropy

24

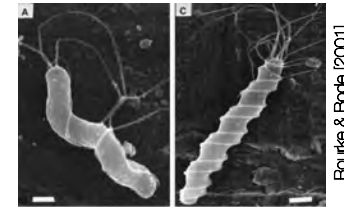
example - persistence length of flagella



Persistence length of flagella Flagella are tail-like structures that project from the cell body of certain prokaryotic and eukaryotic cells. Flagella are hollow cylinders, of the order of $10\mu\text{m}$ long, used for locomotion. Calculate the persistence length A of flagella at room temperature $T = 300\text{K}$. Assume an inner and outer radius of $r^{\text{int}} = 0.07\mu\text{m}$ and $r^{\text{out}} = 0.10\mu\text{m}$, respectively, and a Young's modulus of $E = 1 \cdot 10^8 \text{ J/m}^3 = 1 \cdot 10^8 \text{ N/m}^2$. For hollow cylinders, $I = \pi [r^{\text{out}^4} - r^{\text{int}^4}] / 4$.

3.3 biopolymers - entropy

example - persistence length of flagella



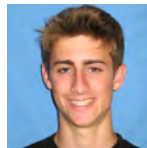
Persistence length of flagella Flagella are tail-like structures that project from the cell body of certain prokaryotic and eukaryotic cells. Flagella are hollow cylinders, of the order of $10\mu\text{m}$ long, used for locomotion. Calculate the persistence length A of flagella at room temperature $T = 300\text{K}$. Assume an inner and outer radius of $r^{\text{int}} = 0.07\mu\text{m}$ and $r^{\text{out}} = 0.10\mu\text{m}$, respectively, and a Young's modulus of $E = 1 \cdot 10^8 \text{ J/m}^3 = 1 \cdot 10^8 \text{ N/m}^2$. For hollow cylinders, $I = \pi [r^{\text{out}^4} - r^{\text{int}^4}] / 4$. Accordingly, $A = [EI] / [kT] = [1 \cdot 10^8 \text{ J/m}^3 \pi [0.10^4 - 0.07^4] \mu\text{m}^4] / [4 \cdot 1.38 \cdot 10^{-23} \cdot \text{J/K} 300 \text{ K}] = 1.44 \text{ m}$. The persistence length of flagella is $A = 1.44\text{m}$. As expected, they are relatively stiff to support cell locomotion.

3.3 biopolymers - entropy

the swimming velocity of mammalian sperm

Final Project ME239, Winter 2011

ME239 FINAL PROJECT
 Sinusoidal model for flagellar motion
 Sean Ramey
 Department of Mechanical Engineering, Stanford University
 Stanford, California



Abstract. Decreasing fertility and the rising fields of micro-fluidics and bio-ministry have led to a more concentrated effort on studying the unique style of motility employed by sperm cells. Since the 1950's, the model developed by Hancock (1953) has been the leader in sperm modeling. This model is accurate but employs many complexities of fluid mechanics. Upon closer observation, the motion of the sperm's tail appears like that of a cork-screw and, when viewed from the side, behaves as a sinusoidal wave that propels the sperm by translating away from its body. When modeled as such, the absolute velocity of the sperm can be very accurately quantified for smaller sperm cells (0% error for human cells) and are within 20% for larger cells, such as those of the Chinese Golden Hamster. This simple model gives a easy and rapid way to quantify different characteristics of sperm cells and ultimately gives a more clear understanding of the methods through which sperm cells move.

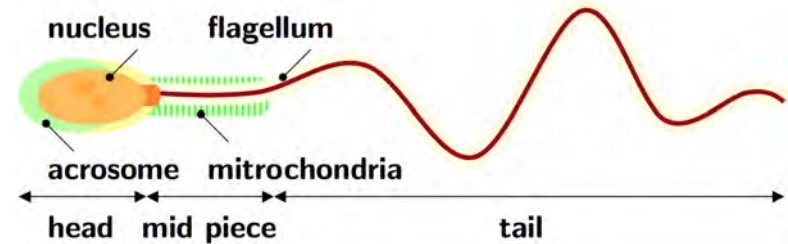


Figure 1. The mammalian sperm consists of a head, a mid piece, and a tail region. The head consists of the nucleus and a cap-like tip, the acrosome. During fertilization, the acrosome secretes lytic substances that break down the walls of the egg. The tail consists of a flagellum, a bundle of nine fused pairs of microtubule doublets surrounding two central single microtubules. The beating of the tail propels the sperm forward at a velocity of approximately 2mm per minute.

example: final project

example: final project

the swimming velocity of mammalian sperm

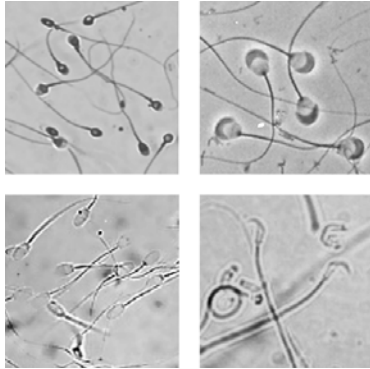


Figure 2. Mammalian sperm cells. Human sperm is slender and thin (top, left). Guinea pig sperm has a head that is four times bigger than the head of human sperm (top, right). Ram sperm has similar size characteristics as human sperm with all dimensions being approximately one third larger (bottom, left). Hamster sperm has a tail that is five times longer than the tail of human sperm and a characteristic hook-shaped head (bottom right).

example: final project

the swimming velocity of mammalian sperm

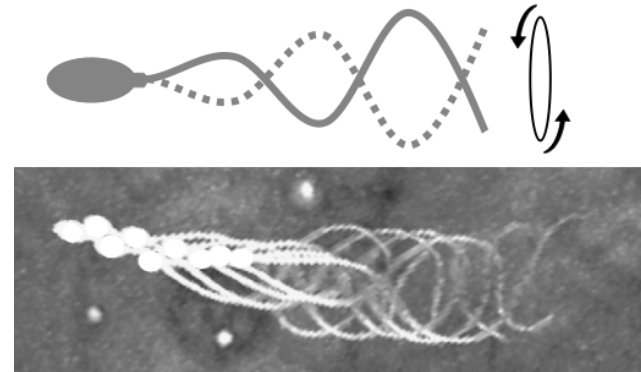


Figure 3. Sperm swimming powered by flagellar beat. The spiraling flagellum generates a sinusoidal wave, which travels away from the head, propelling the sperm through the medium (top). Superimposed images recorded at 20 ms intervals illustrate sperm movement (bottom). Ishijima [2011]

example: final project

the swimming velocity of mammalian sperm



newton's third law: force equilibrium on swimming sperm

$$F_{\text{drag}} - F_{\text{propulsion}} \doteq 0$$

drag on head and normal and tangential propulsion

$$F_h - F_n - F_t \doteq 0$$

example: final project

the swimming velocity of mammalian sperm

drag force on sperm head

$$F_h = \frac{1}{2} C_h \rho v^2 A_h$$

normal and tangential drag forces on sperm tail

$$F_n = \frac{1}{2} C_n \rho v_n^2 A_n \quad \text{with} \quad v_n = v_f \sin \alpha$$

$$F_t = \frac{1}{2} C_t \rho v_t^2 A_t \quad \text{with} \quad v_t = v_f \cos \alpha$$

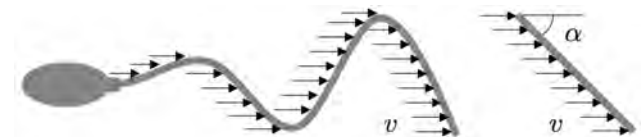
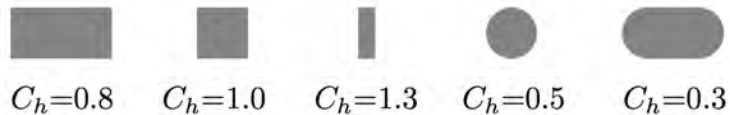


Figure 4. Modeling assumption of flagellar beat. We approximate the flagellum as a sine wave traveling through the fluid in which the sperm is moving (left). We approximate the sinusoid as an unwrapped straight line, inclined at an angle of attach α against the direction of motion (right).

example: final project

the swimming velocity of mammalian sperm



drag of head	normal drag	tangential drag
modeled as bullet	resistive force theory $C_n/C_t \approx 2$	laminar flow over flat plate
$C_h = 0.3$	$C_n = 0.002$	$C_t = 0.001$

Figure 5. Drag coefficients for rectangular, square, plate-shaped, spherical, and bullet-shaped objects in horizontal flow. We approximate the sperm head as bullet-shaped with a drag coefficient of $C_h = 0.3$.

example: final project

33

the swimming velocity of mammalian sperm

$$C_h A_h v^2 - [C_n A_n \sin^2 \alpha + C_t A_t \cos^2 \alpha] v_f^2 \doteq 0$$

correlation of flagellum and sperm velocities

$$v_f = f \lambda - v$$

quadratic equation for sperm velocity v

$$v^2 + 2 \eta f \lambda v - \eta f^2 \lambda^2 \doteq 0 \quad v = [\sqrt{\eta^2 + \eta} - \eta] f \lambda$$

in terms of geometric coefficient η

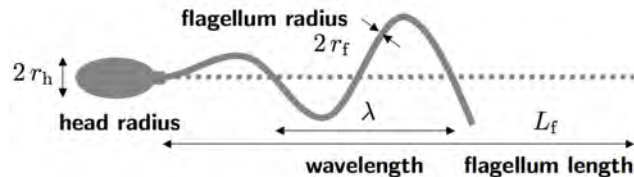
$$\eta = \frac{C_n \sin^2 \alpha A_n + C_t \cos^2 \alpha A_t}{C_h A_h - C_n \sin^2 \alpha A_n - C_t \cos^2 \alpha A_t}$$

The swimming velocity equation is a simplified relationship that correlates the sperm velocity to the flagellum length, the beat frequency, the flagellum wavelength, the flagellum radius, the head radius, and the angle of attack. It describes the steady-state velocity of a flagellum-propelled mass using the basic equations of fluid mechanics.

example: final project

34

the swimming velocity of mammalian sperm



	length $L_f (\mu\text{m})$	frequency $f (\text{Hz})$	wavelength $\lambda (\mu\text{m})$	radius $r_f (\mu\text{m})$	radius $r_h (\mu\text{m})$
human	45	14	32	0.25	1.25
guinea pig	98	22	86	0.25	4.70
ram	59	29	55	0.23	1.64
hamster	260	14	130	0.40	2.00

Figure 6. and Table 2. Characteristic dimensions of mammalian sperm cells. Flagellum length, frequency, wavelength, flagellum radius, and head radius for human, guinea pig, ram, and hamster.

example: final project

35

the swimming velocity of mammalian sperm

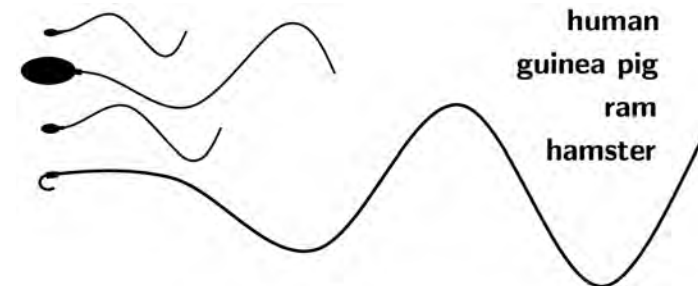


Figure 7. Characteristic dimensions of mammalian sperm cells. Human sperm is slender and thin. Guinea pig sperm has a head that is four times bigger than the head of human sperm. Ram sperm has similar size characteristics as human sperm with all dimensions being approximately one third larger. Hamster sperm has a tail that is five times longer than the tail of human sperm and it has a characteristic hook-shaped head.

example: final project

36

the swimming velocity of mammalian sperm

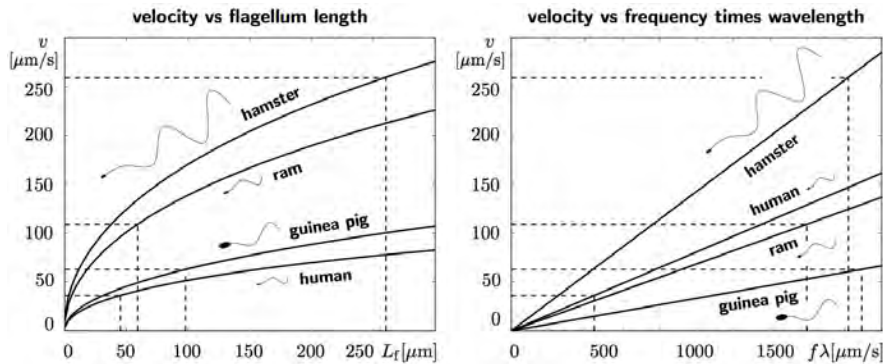


Figure 8a. Sensitivities of human, guinea pig, ram, and hamster sperm velocities with respect to flagellum length (left) and frequency times wavelength (right). Sensitivities are calculated with three out of four parameters fixed to their physiological values, while the fourth parameter is varied.

example: final project

37

the swimming velocity of mammalian sperm

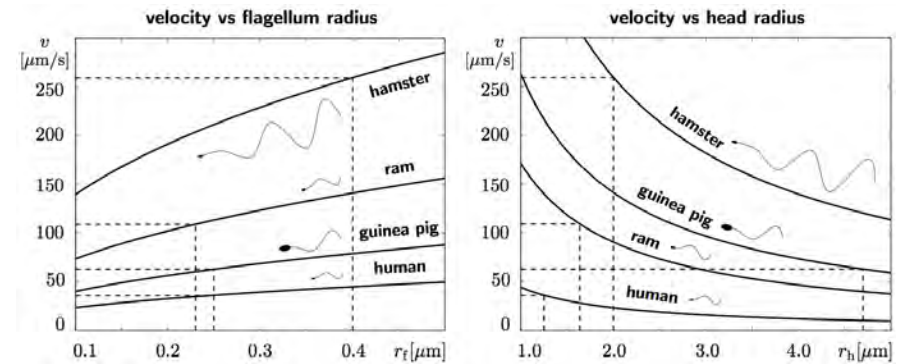


Figure 8b. Sensitivities of human, guinea pig, ram, and hamster sperm velocities with respect to flagellum radius (left) and head radius (right). Sensitivities are calculated with three out of four parameters fixed to their physiological values, while the fourth parameter is varied.

example: final project

38

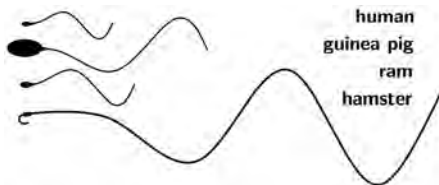
the swimming velocity of mammalian sperm

sperm force

$$F = \frac{1}{2} C_h \rho A_h v^2$$

sperm power

$$P = F v$$



	sperm velocity [$\mu\text{m/s}$]	sperm force [fN]	sperm power [fN $\mu\text{m/s}$]	force per length [fN/m]	measured velocity [$\mu\text{m/s}$]	modeling error [%]
human	36	0.0009	0.04	22	36	0
guinea pig	63	0.0422	2.66	431	75	16
ram	109	0.0154	1.69	262	136	20
hamster	259	0.1303	33.82	501	320	20

Table 3. Characteristic velocities of mammalian sperm cells. Modeled sperm velocity, force, power, and force per length vs measured velocity and modeling error for human, guinea pig, ram, and hamster.

example: final project

39

the swimming velocity of mammalian sperm

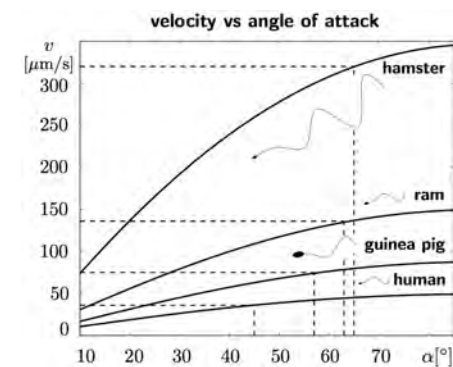


Figure 9. Sensitivities of human, guinea pig, ram, and hamster sperm velocities with respect to angle of attack

example: final project

40